Prabha Materials Science Letters
Vol. 5, No. 2, 412-431, 2026
https://doi.org/10.33889/PMSL.2026.5.2.023

Thermodynamically Simulating Cold Thermal Energy Storage (CTES) System with Encapsulation of Phase Change Material (PCM)

Hemlata Deolal
Department of Mechanical Engineering,
DIT University, 248001, Dehradun, Uttarakhand, India.

Prashant Raturi
Department of Mechanical Engineering,
Swami Rama Himalayan University, Dehradun, Uttarakhand, India.

Sanjeev Kimothi
Department of Physics,
Graphic Era (Deemed to be University), 248002, Dehradun, Uttarakhand, India.
Corresponding author: sanjeevkimothi.phy@geu.ac.in

(Received on September 23, 2025; Revised on May 10, 2026 & June 22, 2026; Accepted on July 13, 2026)

Abstract
Maintaining persistence thermal efficiency during charging of a Cold Thermal Energy Storage (CTES) system is challenging process. In this study CTES thermal efficiency has been examined with assimilation of packed bed mechanism in a cylindrical capsule filled with phase-change material (PCM). A Numerical model is employed with assimilation of energy balance and Heat Transfer Fluid equations. The Temperature of PCM, total energy stored, solidified mass fraction of the tank, effective mass flow rate and heat exchange processes are examined under various thermal stress conditions. The variables used are: processing time frame (0 to 13.5hr), mass fraction (1000kg/hr), Thermal conductivity of the capsule wall (k_c = 0.15-2.5W/mK), Thermal conductivity of material used (k_s = 2.22-3.2 W/mK), diameter of the capsules (dc = 7.7-10cm) and length of capsule (l = 1dc to 4dc). Flow rate, Heat Transfer, and diameter are simulated for the complete solidification time of material, energy stored in the tank and solidified mass fraction during the process. Furthermore, the effect of thermal conductivity of PCM and length of capsule is simulated with the energy storage and solidified mass fraction of the tank. It is observed that all the examined parameters affect the latent heat of storage system and enhanced the energy storage performance of proposed system. This proposed energy storage system will be helpful in conserving heat energy and utilizing as a substitute of electric energy in challenging environment.

Keywords- Thermal energy storage, Phase change material, Heat transfer, Thermal conductivity.

1. Introduction
Due to rising energy consumption and the need to mitigate the effects of climate change by using renewable energy sources, energy storage systems are becoming more and more common in today's society (Mitali et al., 2022; IPCC, 2022). Thermal energy can be preserved and used in place of electrical energy with the aid of a Cold Energy Storage (CTES) system (Sidik et al., 2018; Ali et al., 2024). In particular, the refrigeration system needs to reduce its electrical load and provide cooling during emergencies. To support any additional cooling loads that might be needed, these systems can be employed in conjunction with ones that are already in place (Zarei et al., 2022). Sensible heat storage, latent heat storage, combination storage techniques, and different PCM physical properties control CTES systems. Installing a new cooling load without altering the current air conditioning system is one of the most advantageous applications of CTES (Ruddell et al., 2014; Selvnes et al., 2021). Water, on the other hand, is frequently utilised PCM due to its high latent heat of freezing, low cost, and minimal environmental harm (Zarajabad and Ahmadi, 2018; Barthwal et al., 2021). Several researchers carry out

an experimental study to describe the freezing and melting processes for water in spherical elements (Tan et al., 2009; Chandrasekaran et al., 2015; Adref and Eames, 2022). Spherical encapsulations are better for simulating heat transfer if a suitable thermal conductivity can be discovered to mimic the natural convection taking place within the PCMs (Amin et al., 2014). The super-cooling mechanism is caused by a single nodule containing phase-change material interacting with its crystallisation (El Omari and Dumas, 2004). A semi-empirical formula that predicts the mass of ice inside a sphere at any time was needed for theoretical analysis. This also gives the range of phase change influence, the period of sustainability, and the crystallisation dynamics. to have a better understanding of how the upper nodule within two superposed nodules was impacted by the crystallisation of the bottom nodule. There is a wealth of information on packed bed studies, many of which make use of porous media to forecast flow behaviour and heat transfer properties in bedding layers (Regin et al., 2009). Rocks, pebbles, non-spherical metal, concrete, and other materials can be used as bedding layers (Singh et al., 2010). N-tetradecane was first used as a PCM and in thermal efficiency simulations of a packed bed CTES system by Wu et al. (2010). One-dimensional flow, the lack of axial conduction or dispersion, constant PCM properties, the absence of mass transfer, heat loss to the environment, and the absence of temperature gradients within the solid particles are fundamental model assumptions (Singh et al., 2021). In order to investigate the impact of various parameters on the performance of encapsulated phase change energy storage throughout the charging and discharging processes, a number of tests were conducted (Bilir and Ilken, 2005; Pellicer et al., 2018). Spherical capsules containing water and a PCM nucleation agent were placed within the thermal storage tank. The heat transfer fluid was an aqueous solution of monoethylene glycol that cycled throughout the tank and around the capsules. The industrial process of energy storage is analysed using a two-dimensional model that considers the sub-cooling phenomenon (Kousksou et al., 2005; Bedecarrats et al., 2009). According to the findings, the vertical posture produces the best outcomes in the experimental data. Using a packed bed consisting of spherical capsules filled with phase change materials during the charging and discharging operation, the thermal performance of a latent CTES system was investigated (Kousksou et al., 2008; Beemkumar et al., 2017). N-tetradecane served as the PCM, and HTF was a 40% volumetric concentration of aqueous ethylene glycol solution. The addition of stainless steel, copper and a new PCM-graphite composite material, three strategies were introduced to enhance heat transfer in a cold storage (Chen et al., 2000; Cabeza et al., 2002; Zarei et al., 2022). These processes used water/ice as a PCM and observed that the heat flow increased more noticeably with the PCM-graphite composites and PCM-capsule in cold thermal storage. A high-performance liquid phase cold storage system and liquid air energy storage has been designed and tested for large-scale use in supercritical compressed air energy storage systems (Fang et al., 2016; Sathishkumar and Cheralathan, 2023; Sundaram et al., 2023; Guo et al., 2024; Sathishkumar et al., 2024). Materials for thermal energy storage in solar powered equipments and building applications are tested for both transient and steady-state thermal performance (Niu et al., 2024; Kumar et al., 2025). An experiment of the liquid air energy storage systems packed bed cold energy storage is carried out for the evaluation of the combined heating and power generating capabilities of liquid air energy storage with improved cold storage density (Zarei et al., 2022; Peng et al., 2023; Wang et al., 2024). For energy storage system applications, a numerical analysis of the cyclic cold storage performance in a solid-packed bed tank has been tested (Eames and Adref, 2002, Cárdenas-Ramírez et al., 2022; Sharma et al., 2023). Thermodynamic analysis of adiabatically compressed liquid air has been investigated, and it has been proposed that high temperature sensible thermal energy storage is an essential component of Carnot batteries. In order to produce energy consistently and effectively while utilising resources, a packed-bed latent thermal energy storage system (PLTES) is necessary. It has several potential uses in the improvements in packed-bed design and PCM encapsulation (Cheng et al., 2018).

To meet the growing thermal energy demands of high-power devices are required increasing efficiency and optimal use of renewable energy sources in order to deliver clean, economical energy (Agbakwuru et al., 2024). The United Nations objective is to ensure that everyone has access to affordable, reliable, sustainable energy, clean cooking fuels, and electricity (McCollum et al., 2017; He et al., 2022a). Conventional single-mode cooling techniques are limited in terms of heat dissipation capacity and system efficiency in order to satisfy the expanding thermal energy management requirements of high-power electronic devices (McCollum et al., 2017; He et al., 2022b). In order to facilitate cooling, thermal management, and the integration of renewable energy sources, cold thermal energy storage (CTES) systems must predict latent heat (Anjum et al., 2026). Phase change materials (PCMs) have attracted a lot of interest due to advantages on capacity to store and release latent heat during reversible phase transitions, and have the potential to revolutionize energy management systems (Vasista et al., 2025). Sun et al. (2025) used thermoelectric cooler as a cold source and numerical simulation to examine the thermal behavior and optimization of a phase change cold energy storage device. Additionally, Liang et al. (2024) examine the effects of a PCM-based CES's charging and discharging procedures as well as encapsulation factors including plate size and fin structure. The varying PCM plate's dimension with a constant volume the reduced the charging and discharging time was reported. The experimental findings show that the CES significantly affects the inlet flow rate and PCM plate arrangement on heat transfer performance. Various researchers (Shi et al., 2017; Jia et al., 2021; Fu, 2026) have studied the thermodynamic and economic efficiency of a Combined Cooling, Heating, and Power (CCHP) system to maximize the use of the energy flow, improve system efficiency, and lower the cost of energy storage for distributed applications of renewable energy. A multi-mode coupled thermal management module that integrates phase change materials (PCM), a three-dimensional pulsating heat pipe (3D-PHP), and a forced air cooling module was examined by Gan et al. (2025) and reported the improve thermal reliability and energy efficiency of the system. This study highlights the module's wide application potential in high heat flux densities and variable operating conditions.

Current study insights into physical dependent characteristics that affect renewable energy storage systems and could be utilized to store heat energy instead of electric energy in the challenging environment. This will be achieved through maximizing renewable energy storage capability, efficiency. This study focused on the simulation of cylindrical encapsulation procedure for analyzing the efficacy of CTES system with various physical dependent elements and storage system specifications. Examining parametric variability and how it behaves with multistep performance is intended to increase the thermal cold thermal energy storage (CTES) system capacity. In challenging conditions, this suggested energy storage technology could be employed to store heat energy instead of electric energy.

2. Material and Methods

The current study focuses on simulating energy storage systems with different physical dependant factors and specifications of storage system. The goal is to examine the parametric variability and their behavior with multistep performance to enhance the capacity of thermal cold energy storage system.

2.1 Mathematical Modeling

The mathematical formulation is carried out by establishing energy balance for the PCM in cylindrical capsules and the HTF. The **Figure 1(a)** depicts the schematic diagram of the packed bed system and demonstrated as the cylindrical tank filled with PCM in cylindrical capsules.

In order to investigate the system following assumptions are taken into account.

1) The tank is vertical, well-insulated, and has a bottom-to-top flow for charging and a top-to-bottom flow for discharging.

2) There is longitudinal and viscous flow in the tank, and the flow is laminar and two dimensional.
3) Radial position has no impact on temperature variation because it mostly happens in the axial direction.
4) The tank has been divided into layers of (n_l), each of which has a length (H/n_l) that is sufficiently short to allow for the assumption that the layer is at a single temperature, i.e. the temperature of PCM and HTF are constant in each layer. The HTF flow is fully developed in axial direction.
5) Sub cooling of ice is neglected.
6) The flat surface area of the capsule is neglected.

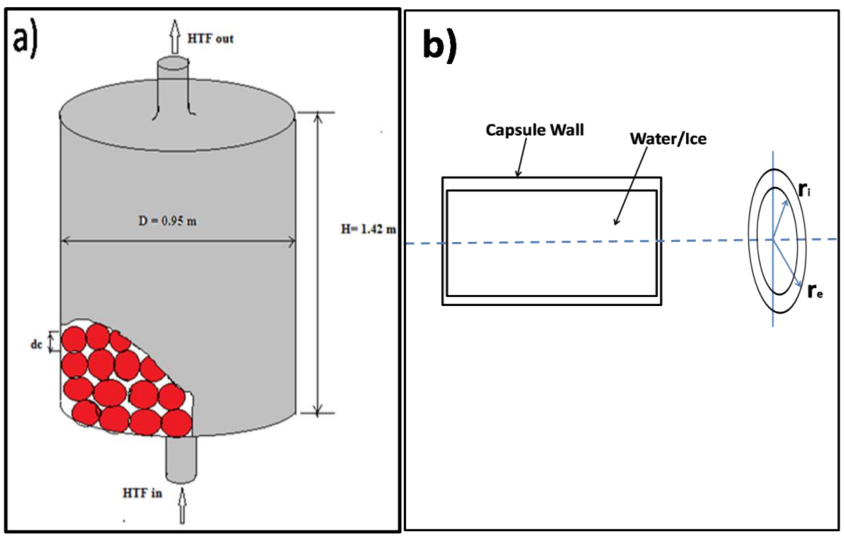

Figure 1. (a) Layout of the storage tank (b) Cross- section of the cylindrical capsule.

The present system consist water in plastic capsules surrounded by coolant; all contained within a cylindrical tank and cross-section of the cylindrical capsule is shown in **Figure 1(b)**. The tank has been divided into a number of layers (n_l), each layer has a number of capsules (n), which is an integer and has a height equal the diameter (dc) of a single capsule. The number of layers (n_l) in the system is calculated through total bed height (H) and capsule diameter dc as: $n_l = \frac{H}{d_c}$.

For creating error free fractional values of n_l an approximate value lower than the actual value can be used. In the present model the important performance parameters are the amount of total energy stored in the tank (E_t), the solidified mass fraction (M_{ft}) and complete solidification time (t) of PCM. Symbols, Greeks letters, subscripts and acronyms used in the study are illustrated in Appendix.

2.2 Charging Process

During the charging process HTF flows over the cylindrical capsules in the packed bed. The PCM in the cylindrical capsules undergoes sensible cooling of liquid phase, solidification of the ice and sub cooling of solid phase. Discharge is accomplished by circulating warm coolant through the tank and past the containers, melting the ice. The energy balance equation for HTF can be written as:

$$\rho_f . Cp_f . V_f . \frac{dT_f}{dt} = \rho_f . Cp_f . q_v (T_{fin} - T_{fout}) + \sum_{i=1}^{n} Q(t) \quad (1)$$

where, ρ_f is the density of HTF (kg/m^3), Cp_f is the specific heat of HTF (J/kgK), V_f is the volume of HTF in each layer (m^3), q_v is the volume flow rate of HTF (m^3/hr), T_{fin} is the inlet layer HTF temperature (degC), T_{fout} is the outlet layer HTF temperature (degC), $Q(t)$ is the heat transfer to or from the capsule (W), and n is the number of capsules in the layer.

Neglecting the first term of the equation because it is too small, so the above energy equation can be written as:

$$\rho_f . Cp_f . q_v (T_{fin} - T_{fout}) = -\sum_{i=1}^{n} Q(t) \tag{2}$$

$$\Rightarrow T_{fout} = T_{fin} + \frac{n.Q(t).3600}{m_f.Cp_f} \tag{3}$$

The energy balance equations for HTF are summarized in different steps:

2.2.1 Sensible Cooling of the Liquid PCM (First Stage)

To evaluate the PCM temperature records during sensible cooling of the liquid PCM, it is assumed that the temperature of the liquid PCM is homogeneous, and the internal energy variation in the PCM is equal to the heat transfer rate from the capsule. The energy balance formation in a cylindrical capsule is illustrated in **Figure 2,** and sensible heat cooling flow process is governed as:

$$\rho_{pcm} . Cp_{pcm} . V_{pcm} . \frac{dT_{pcm}}{dt} = -Q(t) \tag{4}$$

$$\Rightarrow T_{pcmnew} = T_{pcmold} - \frac{Q(t).3600.\Delta t}{\rho_{pcm}.Cp_{pcm}.V_p} \tag{5}$$

Heat transfer between PCM and HTF during sensible heat cooling process is calculated by

$$Q(t) = \frac{T_{pcm} - T_{fin}}{R_f + R_{env}} \tag{6}$$

where, $$R_f = \frac{1}{h.Sc} \tag{7}$$

$$R_{env} = \frac{1}{2.\pi.k_c.\, l} \ln\left(\frac{re}{r_i}\right) \tag{8}$$

where, ρ_{pcm} is the density of PCM (kg/m^3), Cp_{pcm} is the Specific heat of PCM (J/kgK), V_{pcm} is the Volume of PCM in a single capsule (m^3), T_{pcm} is the temperature of PCM inside the capsule (^{0}C), $Q(t)$ is the rate of heat transfer between PCM and HTF (W), T_{fin} is the HTF temperature at the inlet to the layer (^{0}C), R_f is the thermal resistance for convective exchange between the envelope and the fluid (K/W), R_{env} is the thermal resistance of the envelope of the capsule (K/W), h is the heat transfer coefficient between the capsule and HTF (W/m^2 K), s_c is the external surface area of the capsule (m^2), k_c is the thermal conductivity of the envelope of the capsule (W/m K), r_i is the inner radius of the capsule (m), r_e is the external radius of the capsule (m).

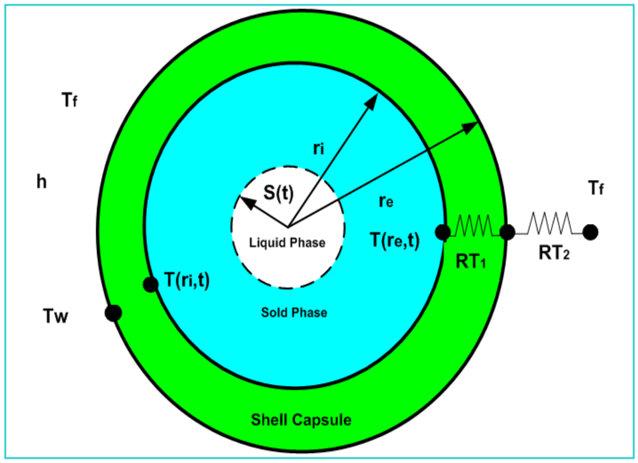

Figure 2. Energy balance system in a cylindrical capsule.

2.2.2 Latent Heat Exchange During Phase Change Process (Second Stage)

When PCM attains the solidification temperature i.e $\mathbf{T_s}$ = 0^0C, solidification process will be started. Heat transfer between PCM and HTF during solidification process is calculated as:

$$Q(t) = \frac{T_s - T_{fin}}{R_f + R_{env} + R_c} \quad (9)$$

$$R_c = \frac{1}{2.\pi.ks.\ l} \ln\left(\frac{ri}{r_c}\right) \quad (10)$$

where, R_c is the thermal resistance of the solid PCM (K/W), r_c is the radius of the solidified ice during freezing and it is calculated by using the heat balance relation (Equation (10)).

$$2\pi.r_c.l.\rho_{pcm_s}.L_F.dr_c = -Q(t)dt \quad (11)$$

These calculations are repeated till r_c = 0.

For heat transfer coefficient is calculated assuming that the main mode of heat transfer is natural convection:

$$Nu = \left(0.60 + \frac{0.387\ Ra^{\frac{1}{6}}}{\left[1+\left(\frac{0.559}{Pr}\right)^{\frac{9}{16}}\right]^{\frac{8}{27}}}\right)^2 \quad (12)$$

$$Ra = \frac{g\beta\rho_f^2 Cp_f(T_{pcm} - T_{fin}) l_c{}^3}{\mu.k_f} \quad (13)$$

$$h = \frac{N_u.k_f}{dc} \quad (14)$$

where, N_u is Nusselt number Ra is Rayleigh number, Pr is Prandtl number, $k_f$is the Thermal conductivity of HTF, g is Gravitational acceleration (m/s^2), ρ_f is the density of HTF (kg/m^3), Cp_f is the specific heat of

HTF (J/kgK), l_c is the characteristic length of the capsule (m), μis the dynamic viscosity of HTF (kg/m.s), k_f is the thermal conductivity of HTF (W/mK).

The amount of energy stored during sensible cooling is calculated by:

$$E_s = m_{pcm,l}.Cp_{pcm}.\left(T_{pcm,new} - T_{pcm,i}\right).n \tag{15}$$

where,$T_{pcm,new}$ is the Temperature of PCM at new time step (^{0}C) and $T_{pcm,i}$is initial PCM's temperature, n is the number of capsules in each layer.

The amount of energy stored during phase change process is calculated by:

$$E_l = \rho_{pcm,s}.\pi.({r_i}^2 - {r_c}^2).l.L_f.n \tag{16}$$

where, E_l is the energy stored in the tank due to solidification process (MJ), $\rho_{pcm,s}$ is the density of solid PCM (kg/m3), r_i is the inner radius of the capsule (m), r_c is the inner radius of the solid PCM (m), L_F is the latent heat of fusion of PCM (J/kg), n is the number of capsule in each layer.

Total amount cold energy stored in the tank is calculated by:

$$E_t = \sum_1^{n_l}(E_s + E_l) \tag{17}$$

where, n_l is the number of the layers in the tank.

The amount of solidified ice in the layer is calculated by:

$$m_s,l = \rho_{pcm,s}.\pi.\left(r_i^2 - r_c^2\right).l.n \tag{18}$$

The amount of the solidified mass fraction of the tank is calculated by:

$$M_{ft} = \Sigma_{n_{l=1}}^{n_l} \frac{m_s,l}{m_t} \tag{19}$$

where, m_t is the total mass of PCM in the tank(kg), $n_l$is the number of the layers in the tank.

3. Results and Discussion

The performance of the system with various influencing parameters such as: mass flow rate of HTF (mf), diameter of the capsules (d_c), thermal conductivity of capsule wall material and thermal conductivity of the PCM and length of capsule during charging process has been investigated. The effect of mass flow rate of HTF is examined along with temperature of PCM, total energy stored in the tank, solidified mass fraction of the tank, time frame (t = 0 to 13.5 hr), mass fraction (mf = 1000 kg/hr), k_c = 0.15-2.5 W/m K, k_s = 2.22-3.2 W/m K, diameter of the capsules (dc = 7.7-10cm), and length of the capsule (l = 1-4 time dc). These procedures are iterated for each cycle of calculation $t_{new} = t_{old} + \Delta t$, till complete solidification has been attained ($r_c = 0$). This time instant t_{new} is called complete solidification time for the given set of parameters. Due to the tiny capsule diameter and predominant axial heat transmission, a 1D axial approximation was used, assuming low radial temperature gradients, even though the physical process is intrinsically 2D. Since their impact on the total thermal response is thought to be negligible under the current operating conditions, sub-cooling and variable surface area effects were disregarded in order to simplify the model. The procedure for heat transfer coefficient calculation is repeated for all possible sets of system parameters, the details of the used constants and variable parameters are summarized in **Tables 1, 2** and **3**. The findings of the numerical simulation for thermal behavior of the packed bed during the charging process have been summarized.

3.1 Thermal Performance of the Bed

Figure 3 illustrates the temperature variations of PCM for fixed values of mass flow rate of HTF and other system parameters. The temperature has decreased to the freezing point (0°C) up to five layers of the bed in about 20 minutes of charging due to the heat transfer between PCM and HTF. After half an hour of charging of PCM, the temperature has reached the freezing temperature up to ten layers of the bed and the entire bed has attained the freezing temperature before 1 hour of charging.

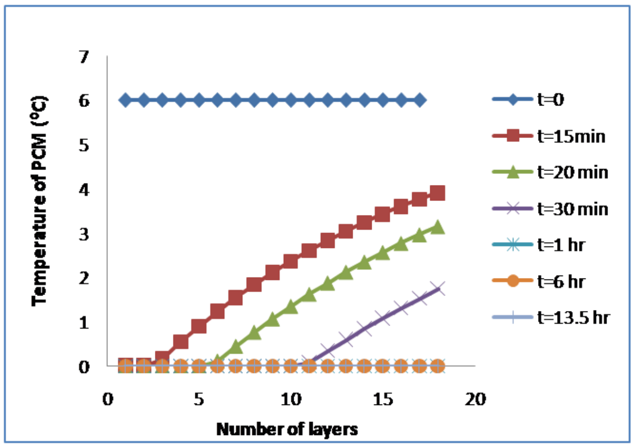

Figure 3. Temperature of PCM along the height of the tank as a function of time.

Figure 4 illustrates the total energy stored in the tank as a function of time. It can be observed from the figure that the energy stored increases with time up to about 13.33 hours of charging; beyond this the value is nearly asymptotic. It is observed that the rate of increase of energy storage is nearly constant because a considerably long time is taken for latent heat release and the entire tank (all capsules) are in the process of freezing during most of the time. **Figure 5** shows variation of solidified mass fraction of the tank with time. It can be seen from the curve that the solid fraction of the tank increases with time up to 13.33 hours of charging which indicate that the entire mass of PCM get frozen.

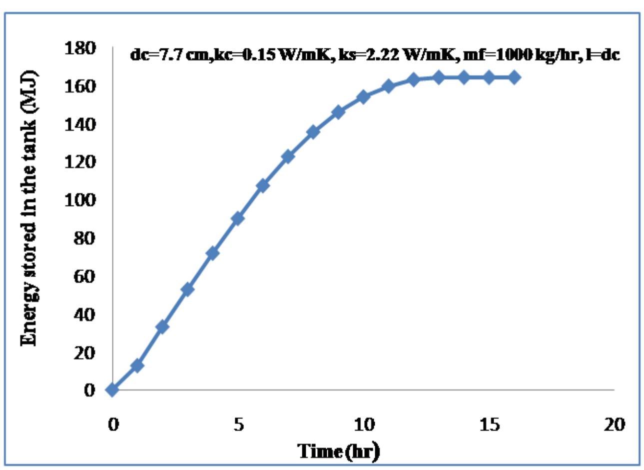

Figure 4. Total energy stored in the tank.

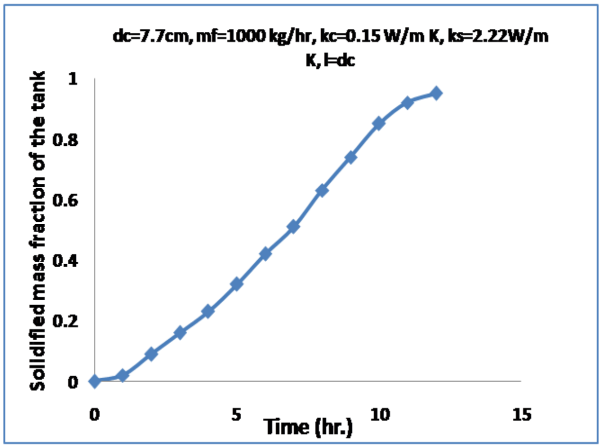

Figure 5. Total solidified mass fraction of the tank.

3.2 Effect of Mass Flow Rate of Heat Transfer Fluid

Figure 6 and **Figure 7** depicts the effect of mass flow rate of HTF on stored cold energy and solidified mass fraction in the tank. The mass flow rate of HTF is varied from 1000 to 2500 kg/hr, while other parameters are kept the same. It is obvious that as a result of increase in flow rate, convective heat transfer coefficient are higher which result in higher values of energy stored as well as higher solidified mass fraction in a given interval of time.

Figure 8 shows the effect of mass flow rate on complete solidification time of PCM. It shows that the time taken for complete solidification of PCM decreases with an increase of mass flow rate of HTF because a higher mass flow rate results in higher velocity and hence higher heat transfer coefficient leading to lower complete solidification time.

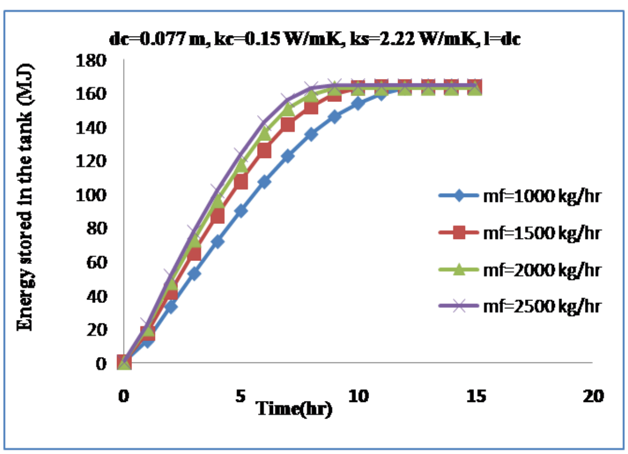

Figure 6. Effect of mass flow rate of HTF on the energy stored in the tank.

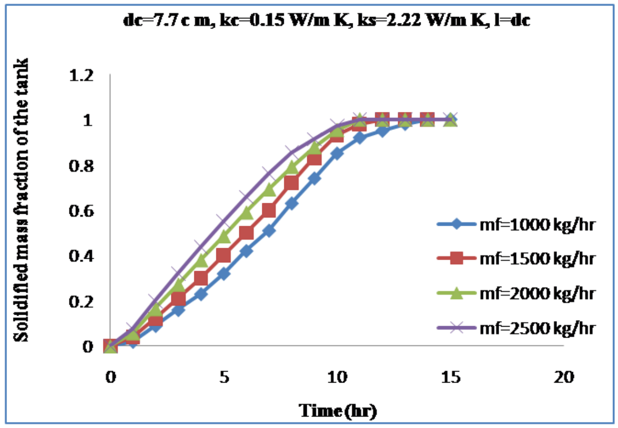

Figure 7. Effect of mass flow rate of HTF on the solidified Mass fraction in the tank.

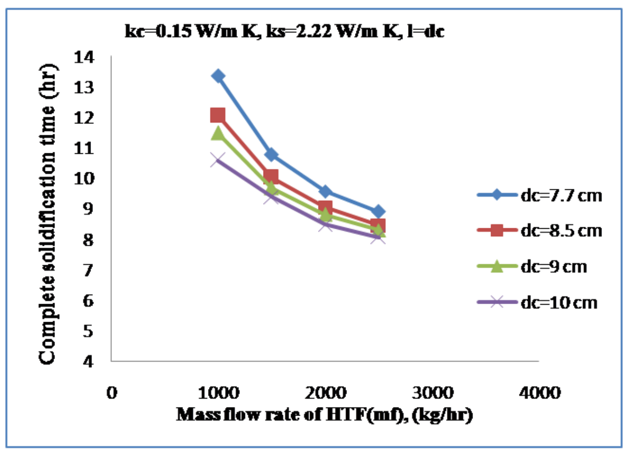

Figure 8. Effect of flow rate of HTF on complete solidification time of PCM at various capsule diameters.

3.3 Effect of Diameter of Capsules

Diameter of capsules has an impact on energy stored capacity is shown in **Figure 9** for fixed values of other parameters. The diameter of the capsules (dc) is varied from 7.7 to 10 cm. It has been observed that energy stored in the bed increases with an increase in diameter of the capsule because of an increase in heat transfer coefficient when diameter of capsule is increased.

Figure 10 shows the effect of diameter of the capsules on the total solidification time of PCM for different values of mass flow rate of HTF. It can be seen that an increase in the diameter leads to decrease in the complete solidification time. Because increase in diameter is responsible for increase of thermal resistance of the envelope but decrease of thermal resistance for convective exchange between the envelope and the fluid due to increase in exposed area and heat transfer coefficient in the exterior of the cylindrical capsule. So heat transfer rate increases because of the dominant convective resistance.

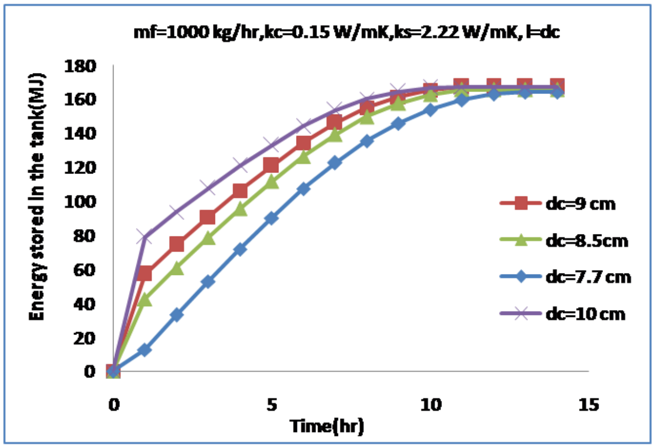

Figure 9. Effect of diameter of the capsules on energy stored in the tank.

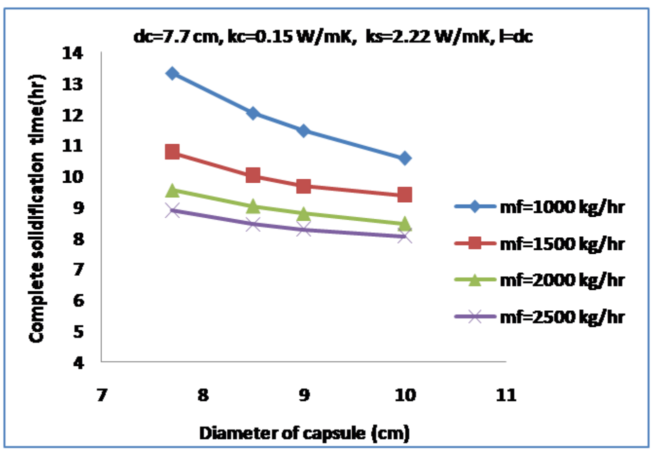

Figure 10. Effect of diameter of the capsules on complete solidification time of PCM.

3.4 Effect of the Thermal Conductivity of the Material of the Capsule Wall

The effect of thermal conductivity of the material of the capsule on the energy stored and solidified mass fraction of PCM is shown in **Figure 11** and **Figure 12** respectively. It can be seen that higher thermal conductivity leads to faster energy storage and solidification because heat transfer rate is increased when the thermal conductivity of capsule wall material is enhanced. It can also be observed that the effect of thermal conductivity almost vanished down beyond a value of around 2.5 W/mK. **Figure 13** depicts the effect of thermal conductivity of capsule wall material on the total solidification time of PCM for different values of 'mf'. In general, the complete solidification time is seen to decrease with an increase of thermal conductivity, the percentage decrease is high in the lower range of values of thermal conductivity (between 0.15 to 1.0 W/mK) whereas the decrease is negligibly small if the thermal conductivity is changed beyond a value of around 2.0 W/m K.

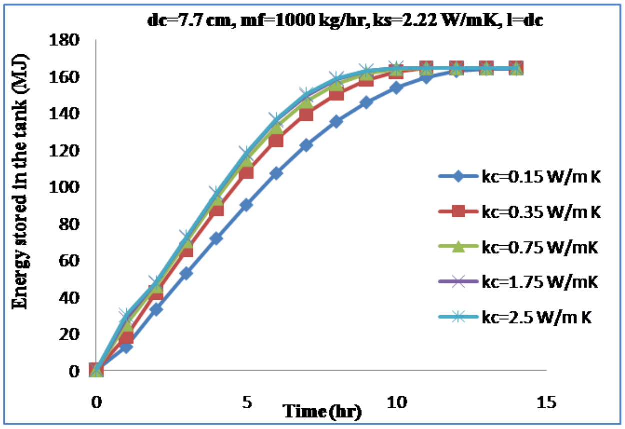

Figure 11. Effect of capsule's material wall on the energy storage in the tank.

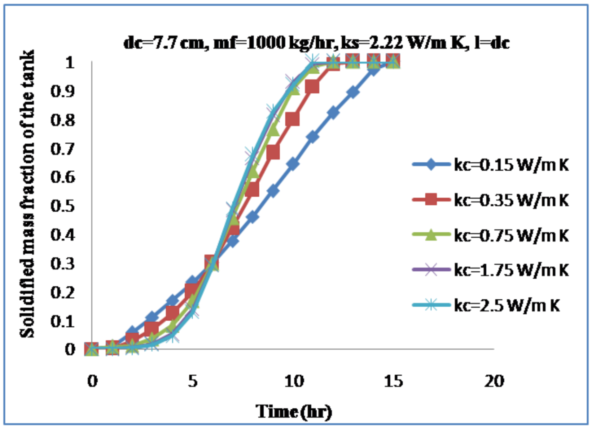

Figure 12. Effect of capsule's wall material on the solidified mass fraction of the tank.

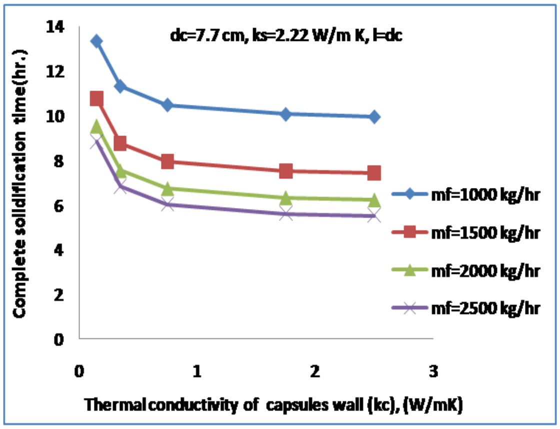

Figure 13. Effect of capsule's material wall on complete solidification time of PCM at various values of mass flow rate of HTF.

3.5 Effect of Thermal Conductivity of PCM

The effect of thermal conductivity of PCM on the energy stored and the solidified mass fraction of the packed-bed has been shown in **Figure 14** and **Figure 15** respectively. The rate of heat transfer to PCM can be substantially enhanced by enhancing the thermal conductivity of PCM. It has been observed that an increase in thermal conductivity results in the enhancement of both the stored energy and solidified mass fraction.

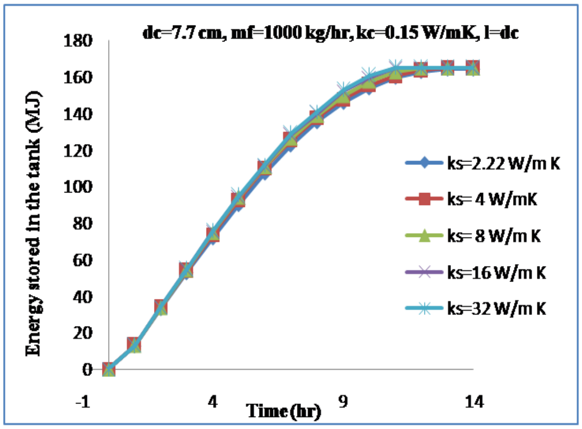

Figure 14. Effect of thermal conductivity of PCM on the energy storage of the tank.

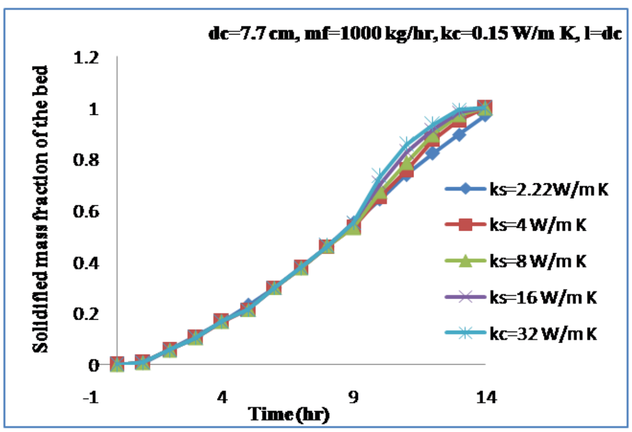

Figure 15. Effect of thermal conductivity of PCM on the solidified mass fraction of the tank.

3.6 Effect of Length of Capsule

Effect of length of capsules on energy stored rate and solidified mass fraction are shown in **Figure 16** and **Figure 17** respectively for fixed values of other parameters. The length of the capsules is varied from 1dc to 4.dc (diameter of capsule is 7.7cm). Energy stored rate and solidified mass fraction rate is higher for larger length of capsule because of an increase in heat transfer rate.

This analysis reveals the simulated effects of HTF flow rate, capsule wall material, and diameter on PCM solidification time, tank energy, and mass fraction of solidified matter. Additionally, the impact of the PCM's thermal conductivity and capsule length on the tank's mass fraction that is solidified and energy storage is explored. It is determined that the properties of the capsule wall material as well as the thermal conductivities of the PCM, dc, and *l* are among the factors that have a significant impact on the latent heat storage and hence affect the system's performance. This process showed that, despite the reduction in length of capsule there is high in the lower range values of thermal conductivity and the higher thermal conductivity of capsule material results in a reduction of the PCM's total solidification time. The effect of capsule length on complete PCM solidification time at various values of HTF mass flow rate signifies that the complete solidification time decreases with the increase of length of the capsule, due to increase in exposed area heat transfer rate increases so complete solidification time decreases as length of the capsule is taken from 1dc to 4dc.

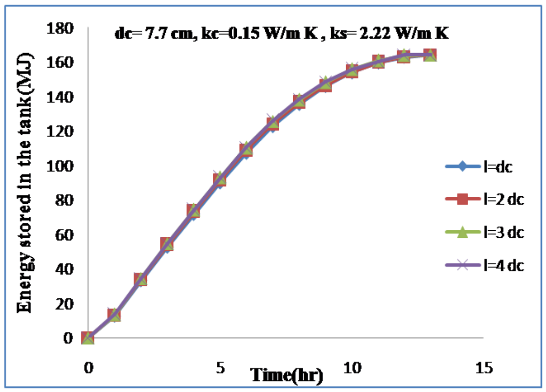

Figure 16. Effect of length of the capsules on energy stored in the tank.

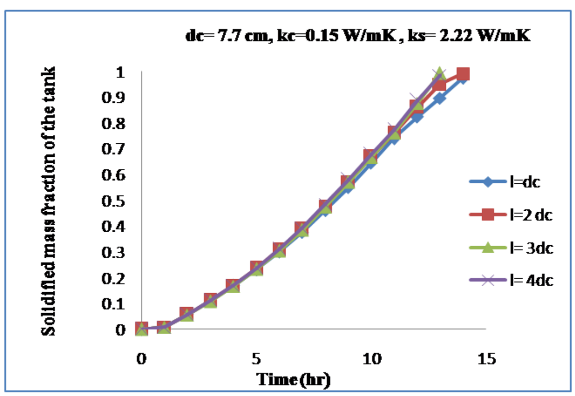

Figure 17. Effect of length of capsule on the solidified mass fraction of the tank.

3.7 Validation with Literature

In order to validate the numerical model comparison was done with the similar studies carried out on the PCM based CTES. According to Cheng et al. (2018) the 24-stage CTES unit with a phase change temperature difference has shown the best thermal performance due to reducing charging time by 15.1% when compared to a single-stage unit, while the quantity and quality of cold charges are nearly identical. The melting properties of PCM inside a CTES tank with interior fins installed are investigated computationally and experimentally by Lee et al. (2023), who also create a 3D mesh system to validate the computational model. The melting of PCM in a finned cold thermal energy storage tank is investigated; the melting process can be greatly influenced by the geometric structures of the fins. To shorten the melt time, increasing fin height works better than increasing fin number. The mean power with the new stratified fin design is 156.3% greater than the power without fins. Bejarano et al. (2018) investigated computationally efficient modelling of PCM-based cold-energy storage systems and proposed that the efficient model should be combined with the refrigeration cycle model in terms of computational cost and accuracy. Relative errors remain below 3% even when the processing effort is reduced by up to 99%. Long-term energy management solutions will be addressed using the proposed paradigm.

4. Conclusions

It might be difficult to keep a CTES system thermally functional during the charging process, but the packed bed mechanism in cylinder capsules filled with PCM is tested for the thermal effectiveness during the charging process of the system. HTF equations and the energy balance are assimilated into a numerical model. The CTES system using packed bed containing cylindrical capsules filled with water as PCM has been numerically simulated to predict the thermal behavior of the system. Parameters that affect strongly the performance of the latent heat storage system include the mass flow rate of heat transfer fluid, thermal conductivities of phase change material and capsule material, diameter and length of the capsule. The time rate of increase of energy storage and the solidified mass fraction increase with an increase of mass flow rate, increase in thermal conductivity of PCM and capsule material and an increase in the diameter and length of the capsules. The complete solidification time decreases with an increase in mass flow rate of heat transfer fluid, thermal conductivity of PCM, thermal conductivity of capsule envelope material, capsule diameter and length to diameter ratio of the capsule. PCM capsules with larger equivalent diameter freeze faster than those with smaller diameter because of the enhancement in heat transfer rate. An increase in thermal conductivity of capsule material results in reduction of complete solidification time, the percentage reduction is high in the lower range of values of thermal conductivities. Both the energy stored as well as solidified mass fraction increase with an increase of thermal conductivity of PCM. This also results in the reduction of complete solidification time. An increase in length to diameter ratio of capsule results in reduction in complete solidification time, but it has weaker dependence in the process of complete solidification time, comparing with other studied parameters. In the context of the futuristic approach, researchers can make use of these results such as complete solidification time to determine the charging time on the basis of simulated values of system and operating parameters or can select suitable values of these parameters to obtain a certain desirable solidification or charging time for their system. Further it can be seen that there is substantial effect of these analyzed parameters on the solidification time.

Appendix

Table 1. Fixed parameters of the system.

No.	Description	Parameter	Value
1.	Height of the tank (m)	H	1.42
2.	Diameter of the tank (m)	D	0.95
3.	Void fraction of the tank	ε	0.4
4.	Inlet coolant temperature (^{0}C)	T_{fin}	-6
5.	Density of the coolant (kg/m3)	ρf	1000
6.	Dynamic viscosity of the coolant (kg/s.m)	μ	$1.422*10^{-3}$
7.	Thermal expansion of the coolant (1/K)	β	$-6.805*10^{-5}$
8.	Density of the PCM (kg/m^3)	ρ_{pcm}	1000
9.	Specific heat of the coolant (J/kg.K)	Cpf	4218
10.	Specific heat of the PCM (J/kg.K)	$Cppcm$	4218
11.	Initial temperature of the PCM (^{0}C)	$Tpcm$	6

Table 2. Nomenclatures used in the study.

Cp_f	Specific heat of HTF, (J/kg K)
dc	Diameter of the capsule, (m)
h	Heat transfer coefficient, (W/m^{2}K)
k_c	Thermal conductivity of the capsule wall, (W/m K)
k_f	Thermal conductivity of HTF, (W/m K)
k_s	Thermal conductivity of PCM, (Wm/K)
L_f	Latent heat of fusion of PCM, (J/kg)
m_f	Mass flow rate of HTF, (kg /hr)
mt	Total mass of PCM in the tank, (kg)
n	Number of capsules in a layer
nl	Number of layers in the tank
Nu	Nusselt number, dimensionless
Pr	Prandtl number, dimensionless
$Q(t)$	Heat transfer to or from the capsule, (W)
qv	Volume flow rate of HTF, (m^3/ hr)
Ra	Rayleigh number, dimensionless
R_{env}	Resistance of the capsule's wall, (K/W)
R_f	Resistance due to convective heat transfer, (K/W)
R_c	Resistance of the solidified ice, (K/W)
r_e	External radius of the capsule, (m)
Sc	Surface area of the capsule, (m^2)
T_{pcm}	Temperature of PCM, (ºC)
T_m	Melting temperature of PCM, (ºC)
T_{fin}	Inlet temperature of HTF, (ºC)
T_{fout}	Outlet temperature of HTF, (ºC)
V_f	Volume of HTF in each layer, (m^3)
V_{pcm}	Volume of PCM inside the capsule, (m^3)
l	Length of the capsule, (m)
GREEK LETTERS	
ρ	Density, (kg/ m^3)
ε	Void fraction, dimensionless
β	Thermal expansion coefficient, (K^{-1})
μ	Dynamic viscosity, (kg s^{-1} m^{-1})
SUBSCRIPTS	
pcm	Phase change material
f	Working fluid
b	Bed
s	Solid
l	Liquid
ACRONYMS	
PCM	Phase change material
HTF	Heat transfer fluid
$CTES$	Cold thermal energy storage

Table 3. Variable parameters of the system.

No.	Description	Parameter	Value
1.	Mass flow rate of HTF (kg/hr.)	mf	1000-2500
2.	Diameter of the capsule (cm)	dc	7.7-10
3.	Thermal conductivity of capsule wall(W/m K)	k_c	0.15-2.5
4.	Thermal conductivity of PCM (W/m K)	k_s	2.22-3.2
5.	Length of the capsule(cm)	l	1dc- 4.dc

Conflicts of Interest
The authors declare that they have no known competing financial interests or personal relationships that could have appeared to influence the work reported in this paper.

Acknowledgments
The authors would like to thank the anonymous reviewer for their insightful feedback on how to make the manuscript better.

AI Disclosure
The author(s) declare that no assistance is taken from generative AI to write this article.

References

Adref, K.T., & Eames, I.W. (2002). Experiments on charging and discharging of spherical thermal (ice) storage elements. *International Journal of Energy Research*, *26*(11), 949-964.

Agbakwuru, V., Obidi, P.O., Salihu, O.S., & MaryJane, O.C. (2024). The role of renewable energy in achieving sustainable development goals. *International Journal of Engineering Research Updates*, *7*(02), 013-027.

Ali, S.A., Habib, K., Younas, M., Rahman, S., Das, L., Rubbi, F., Mulk, W.U., & Rezakazemi, M. (2024). Advancements in thermal energy storage: a review of material innovations and strategic approaches for phase change materials. *Energy & Fuels*, *38*(20), 19336-19392.

Amin, N.A.M., Bruno, F., & Belusko, M. (2014). Effective thermal conductivity for melting in PCM encapsulated in a sphere. *Applied Energy*, *122*, 280-287.

Anjum, S., Khalid, R.Z., Zaman, M., Ishaq, R., & Ullah, A. (2026). Assessment of phase change materials for cooling technologies via data-driven modeling: applications in thermal storage systems. *Applied Thermal Engineering*, 130187.

Barthwal, M., Dhar, A., & Powar, S. (2021). The techno-economic and environmental analysis of genetic algorithm (GA) optimized cold thermal energy storage (CTES) for air-conditioning applications. *Applied Energy*, *283*, 116253.

Bedecarrats, J.P., Castaing-Lasvignottes, J., Strub, F., & Dumas, J.P. (2009). Study of a phase change energy storage using spherical capsules. Part I: experimental results. *Energy Conversion and Management*, *50*(10), 2527-2536.

Beemkumar, N., Karthikeyan, A., & Ramachandran, S. (2017). Heat transfer enhancement of the latent heat storage system using different encapsulating materials with and without fins. *International Journal of Ambient Energy*, *38*(1), 77-84.

Bejarano, G., Vargas, M., Ortega, M.G., Castaño, F., & Normey-Rico, J.E. (2018). Efficient simulation strategy for PCM-based cold-energy storage systems. *Applied Thermal Engineering*, *139*, 419-431.

Bilir, L., & Ilken, Z. (2005). Total solidification time of a liquid phase change material enclosed in cylindrical/spherical containers. *Applied Thermal Engineering*, *25*(10), 1488-1502.

Cabeza, L.F., Mehling, H., Hiebler, S., & Ziegler, F. (2002). Heat transfer enhancement in water when used as PCM in thermal energy storage. *Applied Thermal Engineering*, *22*(10), 1141-1151.

Cárdenas-Ramírez, C., Gómez, M.A., Jaramillo, F., Cardona, A.F., Fernández, A.G., & Cabeza, L.F. (2022). Experimental steady-state and transient thermal performance of materials for thermal energy storage in building applications: from powder SS-PCMs to SS-PCM-based acrylic plaster. *Energy*, *250*, 123768.

Chandrasekaran, P., Cheralathan, M., & Velraj, R. (2015). Influence of the size of spherical capsule on solidification characteristics of DI (deionized water) water for a cool thermal energy storage system–An experimental study. *Energy*, *90*, 807-813.

Chen, S.L., Chen, C.L., Tin, C.C., Lee, T.S., & Ke, M.C. (2000). An experimental investigation of cold storage in an encapsulated thermal storage tank. *Experimental Thermal and Fluid Science*, *23*(3-4), 133-144.

Cheng, X., & Zhai, X. (2018). Thermal performance analysis and optimization of a cascaded packed bed cool thermal energy storage unit using multiple phase change materials. *Applied Energy*, *215*, 566-576.

Eames, I.W., & Adref, K.T. (2002). Freezing and melting of water in spherical enclosures of the type used in thermal (ice) storage systems. *Applied Thermal Engineering*, *22*(7), 733-745.

El Omari, K., & Dumas, J.P. (2004). Crystallization of supercooled spherical nodules in a flow. *International Journal of Thermal Sciences*, *43*(12), 1171-1180.

Fang, G., Tang, F., & Cao, L. (2016). Dynamic characteristics of cool thermal energy storage systems—A review. *International Journal of Green Energy*, *13*(1), 1-13.

Fu, H. (2026). Thermo-economic evaluation of a combined cooling, heating, and power system with photovoltaic-thermal collector and pumped thermal energy storage: a focus on low-grade thermal storage solutions. *Applied Thermal Engineering*, 130952.

Gan, H., Xu, Z., Liu, K., Tian, J.A., Liu, C., & Zhao, J. (2025). Thermal management performance of phase change energy storage/three-dimensional pulsating heat pipe coupled modules under passive and active cooling modes. *Applied Thermal Engineering*, *279*, 127761.

Guo, L., Ji, W., Fan, X., Chen, L., & Wang, J. (2024). Experimental analysis of packed bed cold energy storage in the liquid air energy storage system. *Journal of Energy Storage*, *82*, 110282.

He, J., Yang, Y., Liao, Z., Xu, A., & Fang, K. (2022a). Linking SDG 7 to assess the renewable energy footprint of nations by 2030. *Applied Energy*, *317*, 119167.

He, X., Qiu, J., Wang, W., Hou, Y., Ayyub, M., & Shuai, Y. (2022b). A review on numerical simulation, optimization design and applications of packed-bed latent thermal energy storage system with spherical capsules. *Journal of Energy Storage*, *51*, 104555.

IPCC. Climate Change 2022 - mitigation of climate Change. Cambridge, UK and New York, NY, USA: Cambridge University Press; 2023. https://doi.org/10.1017/ 9781009157926.

Jia, J., Chen, H., Liu, H., Ai, T., & Li, H. (2021). Thermodynamic performance analyses for CCHP system coupled with organic Rankine cycle and solar thermal utilization under a novel operation strategy. *Energy Conversion and Management*, *239*, 114212.

Kousksou, T., Bédécarrats, J.P., Dumas, J.P., & Mimet, A. (2005). Dynamic modelling of the storage of an encapsulated ice tank. *Applied Thermal Engineering*, *25*(10), 1534-1548.

Kousksou, T., Bédécarrats, J.P., Strub, F., & Castaing-Lasvignottes, J. (2008). Numerical simulation of fluid flow and heat transfer in a phase change thermal energy storage. *International Journal of Energy Technology and Policy*, *6*(1-2), 143-158.

Kumar, K.S., Vasanthi, R., Shakir, M., Munimathan, A., Manirathnam, A.S., Alam, M.M., Rajendran, P., & Lee, I.E. (2025). Experimental investigation to enhancing the energy efficiency of a solar-powered Visi cooler. *Scientific Reports*, *15*(1), 18327.

Lee, Y.T., Chien, L.H., Cheung, F.B., & Yang, A.S. (2023). Numerical and experimental investigations on melting heat transfer performance of PCM in finned cold thermal energy storage. *International Journal of Heat and Mass Transfer*, *210*, 124199.

Liang, Y., Yang, H., Wang, H., Bao, X., & Cui, H. (2024). Enhancing energy efficiency of air conditioning system through optimization of PCM-based cold energy storage tank: a data center case study. *Energy*, *286*, 129641.

McCollum, D., Echeverri, L.G., Riahi, K., & Parkinson, S. (2017). Sdg7: Ensure access to affordable, reliable, sustainable and modern energy for all. *A guide to SDG interactions: From Science to Implementation*, 127-173.

Mitali, J., Dhinakaran, S., & Mohamad, A.A. (2022). Energy storage systems: a review. *Energy Storage and Saving*, *1*(3), 166-216.

Niu, J., Zhang, C., Li, Y., Wu, Y., & Sun, H. (2024). Design and investigation of cold storage material for large-scale application in supercritical compressed air energy storage system. *Journal of Energy Storage*, *75*, 109680.

Pellicer, G.B., Vargas, M., Linares, M.G.O., Castaño, F., & Normey-Rico, J.E. (2018). Efficient simulation strategy for PCM-based cold-energy storage systems. *Applied Thermal Engineering*, *139*, 419-431.

Peng, Y., Gao, J., Zhang, Y., Zhang, J., Sun, Q., Du, Q., Tang, Z., & Zhang, T. (2023). Experimental study of adsorption CO2 storage device for compressed CO2 energy storage system. *Journal of Energy Storage*, *58*, 106286.

Regin, A.F., Solanki, S.C., & Saini, J.S. (2009). An analysis of a packed bed latent heat thermal energy storage system using PCM capsules: numerical investigation. *Renewable Energy*, *34*(7), 1765-1773.

Ruddell, B.L., Salamanca, F., & Mahalov, A. (2014). Reducing a semiarid city's peak electrical demand using distributed cold thermal energy storage. *Applied Energy*, *134*, 35-44.

Sathishkumar, A., & Cheralathan, M. (2023). Charging and discharging processes of low capacity nano-PCM based cool thermal energy storage system: an experimental study. *Energy*, *263*, 125700.

Sathishkumar, A., Sundaram, P., Cheralathan, M., & Kumar, P.G. (2024). Effect of nano-enhanced phase change materials on performance of cool thermal energy storage system: a review. *Journal of Energy Storage*, *78*, 110079.

Selvnes, H., Allouche, Y., Manescu, R.I., & Hafner, A. (2021). Review on cold thermal energy storage applied to refrigeration systems using phase change materials. *Thermal Science and Engineering Progress*, *22*, 100807.

Sharma, A., Kothadia, H.B., Singh, S., & Mondal, B. (2023). Solidification of nanoparticle-based PCM in a fin-aided triplex-tube energy storage system for cooling applications. *Thermal Science and Engineering Progress*, *42*, 101872.

Shi, Y., Liu, M., & Fang, F. (2017*). Combined cooling, heating, and power systems: modeling, optimization, and operation*. John Wiley & Sons Ltd, USA.

Sidik, N.A.C., Kean, T.H., Chow, H.K., Rajaandra, A., Rahman, S., & Kaur, J. (2018). Performance enhancement of cold thermal energy storage system using nanofluid phase change materials: a review. *International Communications in Heat and Mass Transfer*, *94*, 85-95.

Singh, D., Gautam, A.K., & Chaudhary, R. (2021). Application of phase change material in building integrated photovoltaics: a review. *Materials Today: Proceedings*, *45*, 4624-4628.

Singh, H., Saini, R.P., & Saini, J.S. (2010). A review on packed bed solar energy storage systems. *Renewable and Sustainable Energy Reviews*, *14*(3), 1059-1069.

Sun, C., Diao, Y., Fang, D., Zhao, Y., Yang, F., Li, Y., Ma, C., & He, W. (2025). Numerical analysis on the thermal behavior and optimization of a phase change cold energy storage device with thermoelectric coolers as a cold source. *Applied Thermal Engineering*, *278*, 127307.

Sundaram, P., Kalaisselvane, A., Sathishkumar, A., Kumar, P.G., Kim, S.C., & Prabakaran, R. (2023). Synthesis, stability, and heat transfer behavior of water and graphene nanoplatelet-based nanofluid for cool thermal storage applications. *Journal of Energy Storage*, *64*, 107219.

Tan, F.L., Hosseinizadeh, S.F., Khodadadi, J.M., & Fan, L. (2009). Experimental and computational study of constrained melting of phase change materials (PCM) inside a spherical capsule. *International Journal of Heat and Mass Transfer*, *52*(15-16), 3464-3472.

Vasista, K.N., Rangarajan, S., & Balaji, C. (2025). Reduced order modeling of minichannel and phase change material based hybrid cooling system: Establishing transient thermal limits. *Applied Thermal Engineering*, *286*, 129331.

Wang, K., Shi, X., & He, Q. (2024). Thermodynamic analysis of novel carbon dioxide pumped-thermal energy storage system. *Applied Thermal Engineering*, *255*, 123969.

Wu, S., Fang, G., & Liu, X. (2010). Thermal performance simulations of a packed bed cool thermal energy storage system using n-tetradecane as phase change material. *International Journal of Thermal Sciences*, *49*(9), 1752-1762.

Zarajabad, O. G., & Ahmadi, R. (2018). Numerical investigation of different PCM volume on cold thermal energy storage system. *Journal of Energy Storage*, *17*, 515-524.

Zarei, A., Seddighi, S., Elahi, S., & Örlü, R. (2022). Experimental investigation of the heat transfer from the helical coil heat exchanger using bubble injection for cold thermal energy storage system. *Applied Thermal Engineering*, *200*, 117559.

Original content of this work is copyright © Ram Arti Publishers. Uses under the Creative Commons Attribution 4.0 International (CC BY 4.0) license at https://creativecommons.org/licenses/by/4.0/

Publisher's Note- Ram Arti Publishers remains neutral regarding jurisdictional claims in published maps and institutional affiliations.